Research Square

Preprints are preliminary reports that have not undergone peer review.
They should not be considered conclusive, used to inform clinical practice,
or referenced by the media as validated information.

Spontaneous Electrical Inversion in Prebiotic Proteinoid Ensembles

Panagiotis Mougkogiannis

pmougoyannis@gmail.com

University of the West of England

Andrew Adamatzky

University of the West of England

Research Article

Keywords:

Posted Date: November 19th, 2026

DOI: https://doi.org/10.21203/rs.3.rs-11367328/v1

License: This work is licensed under a Creative Commons Attribution 4.0 International License.
Read Full License

Additional Declarations: No competing interests reported.

Spontaneous Electrical Inversion in Prebiotic Proteinoid Ensembles

Panagiotis Mougkogiannis[1*] and Andrew Adamatzky[1]

[1*]Unconventional Computing Laboratory, University of the West of England, Bristol, United Kingdom.

*Corresponding author(s). E-mail(s): pmougoyannis@gmail.com;
Contributing authors: andrew.adamatzky@uwe.ac.uk;

Abstract

Negation is the smallest operation that turns a passive conductor of signals into a device capable of logic, because a network that can only copy and combine its inputs cannot compute every Boolean function, whereas one that can also invert them can. We asked whether a purely abiotic material, proteinoid microspheres made by thermal polycondensation of L-glutamic acid, L-phenylalanine and L-aspartic acid, expresses inverting relations between its own sites spontaneously, without any external input. Scanning electron microscopy showed spherical particles 1.4–20.8 µm in diameter with central craters, budding satellites and fused vesicles. Three unstimulated, independently prepared ensembles were recorded on eight differential electrode pairs at 1 Hz, for 69.97 h (recording A), 48.0 h (recording B) and 48.0 h (recording C). In all three, spike-like events coupled between sites only positively: no directed pair showed significant event-triggered suppression. Negation appeared instead at two other levels. First, each recording underwent a slow regime switch that split the electrode pairs into two complementary groups moving in opposite directions. In recording A one site fell by 124 mV and a second rose by 32 mV 2.4 h later (lagged $\boldsymbol{r = -0.94}$), the two binarised potentials were complementary, matching the truth table of negation, in 94.3% of 401 ten-minute bins ($\boldsymbol{p < 0.0005}$); in recording B the leading site rose by 60 mV and another fell by 50 mV 2.6 h later (lagged $\boldsymbol{r = -0.995}$). Second, in recording B one site toggled 199 times between two discrete levels, and at these switches one neighbouring site stepped with it in 91.5% of cases while another stepped against it in 68.8% (both $\boldsymbol{p < 0.0005}$). Third, in recording C five solitary pulses of 5–6 mV at one site were carried with the same sign by two sites and with the opposite sign by a third at every pulse, within minutes ($\boldsymbol{p = 0.018}$ for the inversion against random times). In a fourth sample, stimulated with light switched on and off every 30 min, every responsive site rose when the light came on in

16 to 18 of 18 cycles, and none moved against it. In a fifth sample illuminated with light flickering at 10 Hz in five sessions of different colours, all eight sites followed the flicker, with a phase that was fixed for each site across sessions; one site responded in near anti-phase ($\mathbf{168 \pm 13}^\circ$) to the strongest. We argue that, in proteinoid ensembles, inversion is not a property of single excitations but of the redistribution of a shared, conserved quantity among sites, and that the simultaneous appearance of copying and inverting outputs of one input is a chemical dual-rail representation, the minimal resource from which complete logic can be assembled. Because no input was imposed in the first three recordings, and the leading site in each case was identified after the fact, these relations are spontaneous inversions rather than logic gates, and when an external input was applied the material copied it rather than inverting it.

Keywords: proteinoids, origin of life, unconventional computing, spontaneous inversion, negation, excitable chemical systems, protocells

1 Introduction

Every universal logical basis contains a form of negation. Shannon showed that switching circuits built from relays obey Boolean algebra Shannon (1938), and McCulloch and Pitts showed that threshold units with excitatory and inhibitory inputs can realise any logical expression McCulloch and Pitts (1943). The point that is often left implicit in both accounts is that the inhibitory input, the capacity to say 'not', is what makes the scheme complete. Conjunction and disjunction are monotone operations, and a network built only from monotone operations can never compute a function whose output falls when one of its inputs rises. A system that merely copies, sums or thresholds its inputs is therefore computationally limited in a precise sense, and the first appearance of negation in a material marks the point at which that limit is lifted.

Living systems invert signals everywhere. Repressors silence promoters, phosphatases undo kinases, and inhibitory neurons suppress their targets, and these inverting motifs recur so frequently in cellular networks that they are counted among the basic building blocks of biological regulation Bray (1995); Alon (2007). Synthetic biology confirmed their power by assembling mutual inhibition into a bistable toggle switch Gardner et al (2000) and a ring of three inverters into an oscillator Elowitz and Leibler (2000). Random Boolean networks, introduced to model gene regulation, already assumed that each node could compute an arbitrary function of its inputs, negation included Kauffman (1969). The prebiotic question is therefore not whether negation is useful, but how a chemical system without genes, enzymes or membranes of biological origin first came to express it.

Chemistry offers several routes. Mass-action networks can in principle implement threshold units and therefore Turing-complete computation Hjelmfelt et al (1991). In excitable reaction-diffusion media, the collision and annihilation of travelling waves yields logic gates in which the absence of a wave at an output encodes the presence of a wave at a control input Tóth and Showalter (1995); Steinbock et al (1996); Adamatzky et al (2005); Adamatzky (2019). Strand-displacement cascades build negation with

carefully designed DNA sequences Seelig et al (2006); Qian and Winfree (2011). All of these systems, however, were engineered by people who already knew what a NOT gate is. The origin-of-life setting asks something more demanding, namely whether a chemically plausible material, left to its own dynamics, produces relations between its parts that a logician would recognise as negation Ruiz-Mirazo et al (2014); Mann (2012); Mougkogiannis et al (2026).

Thermal proteinoids are a natural place to look. Fox and Harada showed that heating dry mixtures of amino acids yields protein-like copolymers Fox and Harada (1958), which in water assemble into microspheres that Fox regarded as models of protocells Fox (1988); Mougkogiannis and Adamatzky (2026a,b,c) (Fig. 1). Przybylski and colleagues reported that such microspheres sustain membrane potentials, action-potential-like spikes and oscillations Przybylski et al (1982); Przybylski (1985). Building on these observations, proteinoid ensembles have been proposed as substrates for unconventional computing Adamatzky (2021), and they have been shown to change their electrical responses with stimulation history Mougkogiannis and Adamatzky (2023a) and to implement logical gates when inputs are delivered and outputs are read by the experimenter Mougkogiannis and Adamatzky (2023b). In that earlier work the inputs were imposed. Here no input is imposed at all. We record three unperturbed, independently prepared ensembles of glutamic acid, phenylalanine and aspartic acid proteinoids, for almost three days, two days and two days, and ask whether, among the relations that the material forms between its own electrical sites, there are ones that have the input-output structure of negation.

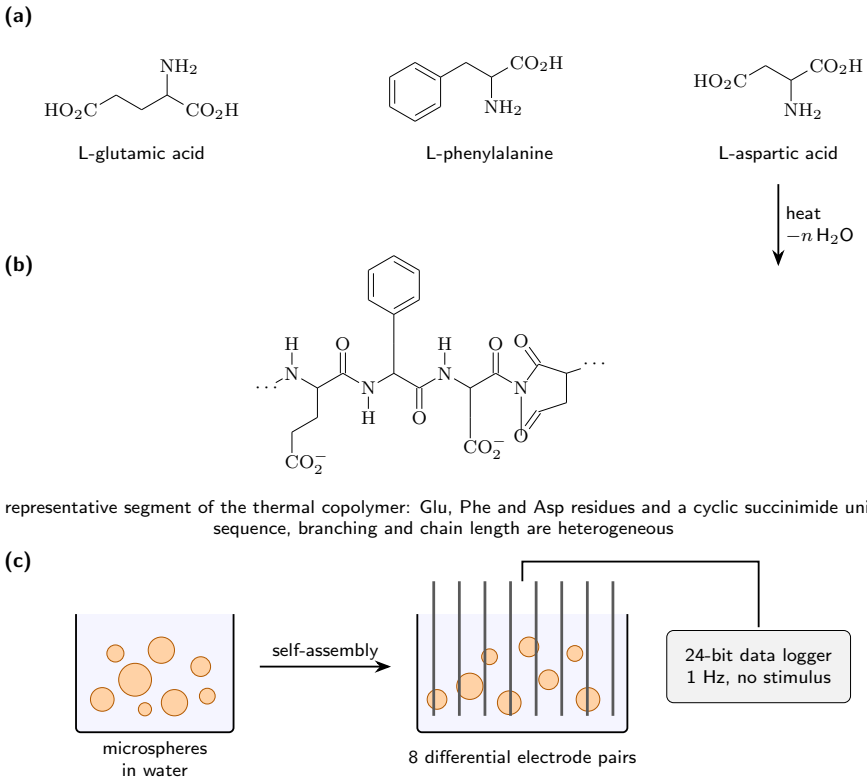


Fig. 1 From amino acids to an excitable ensemble. (a) The three monomers of the Glu–Phe–Asp proteinoid. (b) Thermal polycondensation links them by peptide bonds with loss of water; aspartic acid residues can also close into cyclic succinimide units. The segment shown is representative only, since thermal proteinoids are heterogeneous in sequence, branching and chain length. The carboxylate side chains of glutamic and aspartic acid carry the exchangeable charge invoked in the Discussion. (c) In water the polymer self-assembles into microspheres, whose suspension was recorded with eight differential electrode pairs and no stimulus.

We find evidence for spontaneous electrical inversion; however, its occurrence is strictly timescale- and state-dependent. At the time scale of individual spikes the material copies; it does not invert. Inversion emerges at the time scale of hours, as a slow redistribution of potential in which some regions rise because others fall, and, at the scale of minutes, when a single site switches between two discrete states or emits a solitary pulse. In every case one change is expressed by a copying and an inverting partner at once. We argue that this arrangement is the chemical analogue of dual-rail encoding and is sufficient in principle to bootstrap complete logic. We do not claim, however, that the material implements a NOT gate. A gate requires an input that is set from outside and an output that follows it, whereas here no input was applied, and what we call the input is simply the site that changed first. To see what the material does when an input is imposed, we also recorded a fourth sample while switching a light on and off. Every responsive site followed the light, and none inverted it. A

fifth sample, exposed to light flickering at 10 Hz, showed how a fast imposed input is distributed among sites with different phases.

2 Materials and methods

2.1 Proteinoid synthesis and sample preparation

Proteinoids were prepared by thermal polycondensation of L-glutamic acid, L-phenylalanine and L-aspartic acid following the general procedure of Fox and Harada Fox and Harada (1958), as used in our previous studies Mougkogiannis and Adamatzky (2023a,b). The amino acids were mixed in equal mass proportions, heated under nitrogen at 180 °C for 3 h, cooled, and the product was dispersed in deionised water at a concentration of 5 mg mL^{-1} and allowed to self-assemble into microspheres. The preparation is referred to below as Glu–Phe–Asp, and no other amino acid, salt or additive was included in the sample (the 'pure' formulation). Three independent samples of this formulation were used for the electrical recordings.

2.2 Scanning electron microscopy

A drop of the microsphere suspension was deposited on a fibrous cellulose substrate mounted on an aluminium stub and dried at room temperature. The samples were imaged without a conductive coating, at a low accelerating voltage to limit charging. Images were acquired on a field-emission scanning electron microscope (Quanta FEG, FEI) in high-vacuum mode with the Everhart–Thornley secondary-electron detector, at an accelerating voltage of 1.5–1.6 kV, spot size 1.8 and a working distance of about 2.4 mm, on 1 July 2025. The six fields shown had horizontal field widths between 9.1 and 44.4 µm (pixel sizes 5.9–28.9 nm). Particle diameters were measured by fitting circles to particle outlines with a Hough transform applied to Canny edges, and fits were accepted only after visual confirmation that the circle followed the particle boundary. Seven particles in the six fields yielded an accepted fit; the remaining particles were irregular, fused or too occluded for a reliable outline.

2.3 Electrical recording

Eight pairs of iridium-coated stainless-steel sub-dermal needle electrodes were inserted into the proteinoid suspension with an inter-electrode distance of approximately 10 mm. Each pair was connected to a differential input of a 24-bit data logger (ADC-24, Pico Technology, United Kingdom), so that channel k ($k = 1, \ldots, 8$) reports the potential difference between physical inputs $2k-1$ and $2k$. The input range was ± 2.5 V, and each stored sample is the average of the conversions acquired during one second. Acquisition was controlled with PicoLog 6. Recording A began at 19:30:40 British Summer Time on 7 September 2025 and lasted 69.97 h (251,891 samples per channel); recording B began at 18:45:55 Greenwich Mean Time on 16 February 2025 and lasted 48.0 h (172,802 samples per channel); recording C began at 21:57:05 Greenwich Mean Time on 20 March 2025 and lasted 48.0 h (172,804 samples per channel). No recording contains missing values, and no electrical, chemical or optical stimulus was applied at any time. Channels are labelled A1–A8, B1–B8 and C1–C8. Because the three samples

were prepared and wired independently, channels with the same number in different recordings do not correspond to the same physical location.

2.4 Event detection

Spike-like events were detected on each channel independently. A three-second difference $r(t) = V(t) - V(t-3)$ was computed, and its robust scale was estimated as $\sigma_r = 1.4826\,\mathrm{MAD}(r)$, where MAD is the median absolute deviation Quiroga et al (2004). Samples with $|r(t)| > 8\sigma_r$ were candidate onsets. For each candidate, the slow baseline was removed with a running median of 601 s, and the peak of the baseline-corrected signal within the following 20 s was taken as the event time and amplitude. A candidate was accepted when the peak had the same sign as the onset and its magnitude exceeded both 0.8 mV and six robust standard deviations of the baseline-corrected signal. A dead time of 30 s prevented the same excursion from being counted twice. Event polarity was defined as the sign of the peak amplitude.

2.5 Fast coupling between channels

Directed interactions at the scale of individual events were measured by event-triggered counting. For a trigger channel i and a target channel j, we counted the number C_{ij} of target events falling in the 120 s after each trigger event. To separate genuine fast coupling from shared slow fluctuations in firing rate, the null distribution was generated by jittering every target event independently by a uniform offset in $[-1800, 1800]$ s and recounting, a procedure that preserves rate modulations slower than about one hour while destroying finer temporal structure Grün (2009). One thousand surrogates were drawn for each of the 56 ordered pairs. We report the ratio $R_{ij} = C_{ij}/\langle C_{ij}^{\mathrm{sur}} \rangle$, so that $R_{ij} > 1$ indicates facilitation and $R_{ij} < 1$ indicates suppression, together with a two-sided empirical p-value. The false discovery rate across pairs was controlled with the Benjamini–Hochberg procedure Benjamini and Hochberg (1995). The first 3 h of each recording, during which all channels displayed a settling transient with synchronously elevated activity, were excluded from this analysis. The same procedure applied to a channel against itself, with a window from 30 to 300 s after each event, measured post-event facilitation or refractoriness.

2.6 Slow regimes and Boolean truth tables

For the analysis of slow dynamics, each channel was averaged in non-overlapping 10-s and 10-min bins. No stimulus was applied in any recording. Throughout, ‘input’ denotes the channel whose change came first and ‘output’ a channel that changed afterwards; both labels are assigned after the fact, and they describe temporal order, not experimental control. To compare the relation between an input channel X and a candidate output channel Y with Boolean truth tables, both were binarised. The input was thresholded at the midpoint between its median potential before and after the regime switch described in the Results, and each output was thresholded at its own median over the analysed period. With $x_n, y_n \in \{0, 1\}$ denoting the binary states

in bin n, we define the NOT fidelity and the BUFFER fidelity as

$$F_{\mathrm{NOT}} = \frac{1}{N}\sum_{n=1}^{N} \mathbb{1}\left[y_n = 1 - x_n\right], \qquad F_{\mathrm{BUF}} = 1 - F_{\mathrm{NOT}}. \tag{1}$$

A perfect inverter has $F_{\mathrm{NOT}} = 1$ and a perfect copier has $F_{\mathrm{BUF}} = 1$. Because slow signals are strongly autocorrelated, significance was assessed against 2,000 circular shifts of the output sequence by at least 6 h, which preserve the autocorrelation of each signal while destroying their alignment. Bins from the first 3 h were excluded, leaving $N = 401$ bins in recording A and $N = 270$ in recording B.

A binary agreement can arise trivially when two unrelated signals drift in opposite directions over the whole recording. To distinguish a response to the switch from such drift, we computed for each channel a transition locality index, defined as the difference between its median potential in the 8 h after the switch and in the 8 h before it, divided by the range between its 5th and 95th percentiles over the recording after the first 3 h. The windows were 30–38 h and 46–54 h in recording A, and 26–34 h and 44–48 h in recording B, where the record ends at 48 h. A value near ± 1 indicates that most of the channel's total excursion is concentrated at the time of the switch, whereas a value near zero indicates that any binary agreement is carried by changes elsewhere in the record.

Temporal ordering was established by locating the time at which each signal first crossed the midpoint between its pre- and post-switch levels, and by computing the Pearson correlation between the 10-s series of the leading channel and of each other channel as a function of lag within a window around the switch (34–52 h in recording A, 28–48 h in recording B), for lags up to ± 4 h. Input-output transfer relations were plotted at zero lag and after shifting the output by the lag of maximal absolute correlation. To track when the relation between channels became expressed, Spearman rank correlations were computed between 1-min averages of the input and of each other channel in sliding 6-h windows advanced in 30-min steps.

2.7 Coordination of excitability

To ask whether periods of firing were shared or partitioned between channels, event counts were accumulated in 1-h bins, each channel's hourly count was binarised at its own median, and Eq. (1) was applied to the resulting sequences, with significance assessed by 5,000 circular shifts of at least 6 h.

2.8 Discrete switching events

Channel B8 alternated between two discrete levels during the first 16 h of recording B. Its state was defined as 'up' when its potential exceeded -20 mV, and a 21-s running median removed state flickers shorter than about ten seconds. Each change of state after the first 3 h was taken as a switching event, with sign $s = +1$ for an up switch and $s = -1$ for a down switch. For every other channel j, the step Δ_j associated with a switch was the median potential in the 30 s starting 5 s after the switch minus the median in the 30 s ending 5 s before it. The sign agreement F_{BUF} is the fraction of

switches with $\mathrm{sign}(\Delta_j) = s$, and $F_{\mathrm{NOT}} = 1 - F_{\mathrm{BUF}}$. The null distribution was obtained from 2,000 sets of random times drawn uniformly between 3 and 16 h, each paired with a random permutation of the observed switch signs.

2.9 Solitary pulses

Recording C contained a small number of solitary slow pulses. Its signals were averaged in 10-s bins and band-pass filtered between periods of 10 min and 4 h with a zero-phase second-order Butterworth filter. To avoid selecting outputs together with the input, pulses were defined on C1 alone, as peaks of its robustly z-scored band-passed signal exceeding 3 in absolute value and separated by at least 1 h, between 3 and 47 h; each pulse was given the sign s of its peak. For every other channel j, the response to a pulse was the Pearson correlation between the band-passed C1 and Cj in a $\pm$1-h window around the peak, and its amplitude was the extreme value of the linearly detrended 10-s signal within $\pm$30 min, multiplied by s. The sign agreement F_{BUF} is the fraction of pulses with positive correlation. The null distribution was obtained from 2,000 sets of random times, each paired with a random permutation of the pulse signs, so that it measures how often Cj agrees with C1 at arbitrary moments rather than at pulses. The lag of each response was taken as the shift, within $\pm$15 min, that maximised the absolute correlation.

2.10 Light stimulation

A fourth, independently prepared proteinoid suspension (recording D) was recorded with the same logger from 08:20:02 Greenwich Mean Time on 24 February 2023 for 120.0 h (432,002 samples per channel), on seven differential channels (D1 and D3–D8). Two of them, D6 and D7, read within a few microvolts of zero throughout, apart from occasional saturating glitches, and were treated as non-functional inputs. The suspension was illuminated by a white-light source that was switched on and off at intervals of 30 min during the working hours of 27 and 28 February 2023, and kept in its resting state at other times. No light sensor was recorded, so the transitions were located on D1, where each produced an abrupt change of slope: the 3-min change of the 1-min averaged potential was robustly z-scored, peaks above 6 and below -6 were taken as onsets and offsets of the rising and falling phases, and each onset was paired with the next offset. We take the rising phase as the illuminated one. Reversing this assignment would reverse the sign of every channel's response together, and would therefore not create a pair of sites responding in opposite directions. Eighteen illuminated periods of 26–33 min were obtained, nine on each day; an irregular sequence of transitions in the first 9 h of the recording, during the settling transient, was excluded. For each channel and onset, the step was the median potential in the 5 min starting 30 s after the onset minus the median in the 5 min ending 30 s before it, and offsets were treated in the same way. The fraction of onsets with a rising step was compared with 2,000 sets of random times drawn within the same two working days.

2.11 Periodic light at 10 Hz

A fifth proteinoid suspension (recording E) was monitored on eight channels (E1–E8) during five successive illumination sessions. Each session used continuous flickering light at a nominal frequency of 10 Hz. The sequence was white (from 4 April 2025), red (7 April), blue (9 April), yellow (11 April) and white again (from 16 April). The analysis covered 48 h per session. Only the first 48 h of the final white-light session were included. A sixth session, annotated as a different preparation, was excluded. Each stored sample represents a one-second average. Flicker slightly away from 10 Hz therefore appears as an alias in the recordings. All 40 channel–session combinations showed a sharp spectral line at $f_0 = 0.395241$ Hz and its harmonics. No corresponding line was detected in the unstimulated recordings A–C. The light-locked response was quantified by lock-in demodulation. The first 3 h of each session were excluded. Each record was high-pass filtered by subtracting a 31 s moving average. The filtered signal was then multiplied by $e^{-2\pi i f_0 t}$ and averaged over 10 min windows. Twice the modulus of this average gave the observed amplitude. Noise was estimated using the same procedure at $f_0 \pm 0.013$ Hz and $f_0 \pm 0.020$ Hz. One-second averaging attenuates the true amplitude by a factor of approximately 30. Amplitudes are therefore reported as observed. Channel phases were referenced to E2, which showed the largest response. Relative phases were summarised by their mean resultant across the 10 min windows. No light sensor was recorded. The phase of the illumination therefore remained unknown.

All analyses were performed in Python with NumPy, SciPy and scikit-image, and the code is provided with the article.

3 Results

3.1 Microsphere morphology

Scanning electron microscopy showed that the Glu–Phe–Asp preparation consists predominantly of discrete spherical particles resting on and among the fibres of the substrate (Fig. 2). The seven particles with an accepted circle fit had diameters between 1.4 and 20.8 µm, with a median of 5.6 µm. The larger microspheres carried a central crater or dimple, surrounded in some cases by concentric relief (Fig. 2a–c), a shape consistent with the partial collapse of a hollow or soft-cored particle on drying. Small nodules were scattered over otherwise smooth shells (Fig. 2c). Several particles had satellite spheres budding from their surface or fused to a neighbour (Fig. 2a,b,d), one field contained a short chain of budding spheres of decreasing size (Fig. 2e), and another a cluster of fused, irregular vesicles beside a large microsphere (Fig. 2f). The ensemble probed by the electrodes is therefore a dense, heterogeneous population of micrometre-sized compartments that can bud, fuse and deform, rather than a uniform suspension.

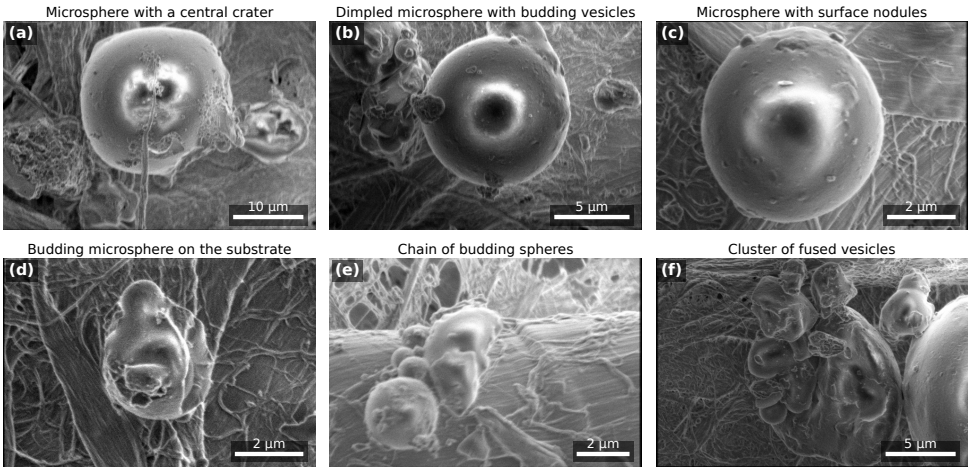


Fig. 2 Scanning electron micrographs of uncoated Glu–Phe–Asp proteinoid microspheres (1.5–1.6 kV, secondary electrons). (a) A microsphere of about 21 µm with a central crater, next to a fused neighbour. (b) A dimpled microsphere of about 10 µm with budding vesicles. (c) A microsphere of about 6 µm with surface nodules. (d) A budding microsphere among the substrate fibres. (e) A chain of budding spheres. (f) A cluster of fused vesicles beside a large microsphere. Scale bars are drawn from the pixel size recorded by the instrument.

3.2 Two excitable ensembles with heterogeneous sites

The eight channels of recording A differed in baseline potential, drift and activity over the 70 h of recording (Fig. 3). Mean potentials ranged from −117.3 mV on A2 to +86.5 mV on A1, and every channel displayed a settling transient during the first two to three hours. Superimposed on these slow trends were brief excursions with a rapid onset and a slower, approximately exponential return (Fig. 4a). Across the ensemble, 4,461 events were detected, between 175 on A6 and 1,129 on A2. Inter-event intervals were broadly distributed, with median values between 65 s on A1 and 383 s on A6 and coefficients of variation between 1.4 and 11.2, so that firing was irregular and clustered rather than periodic. Recording B, shown in Sect. 3.6, was similar in character, with 4,950 events, but activity there was concentrated on four channels (B1, B2, B5 and B8, each with more than 1,000 events), while B6 and B7 were nearly silent.

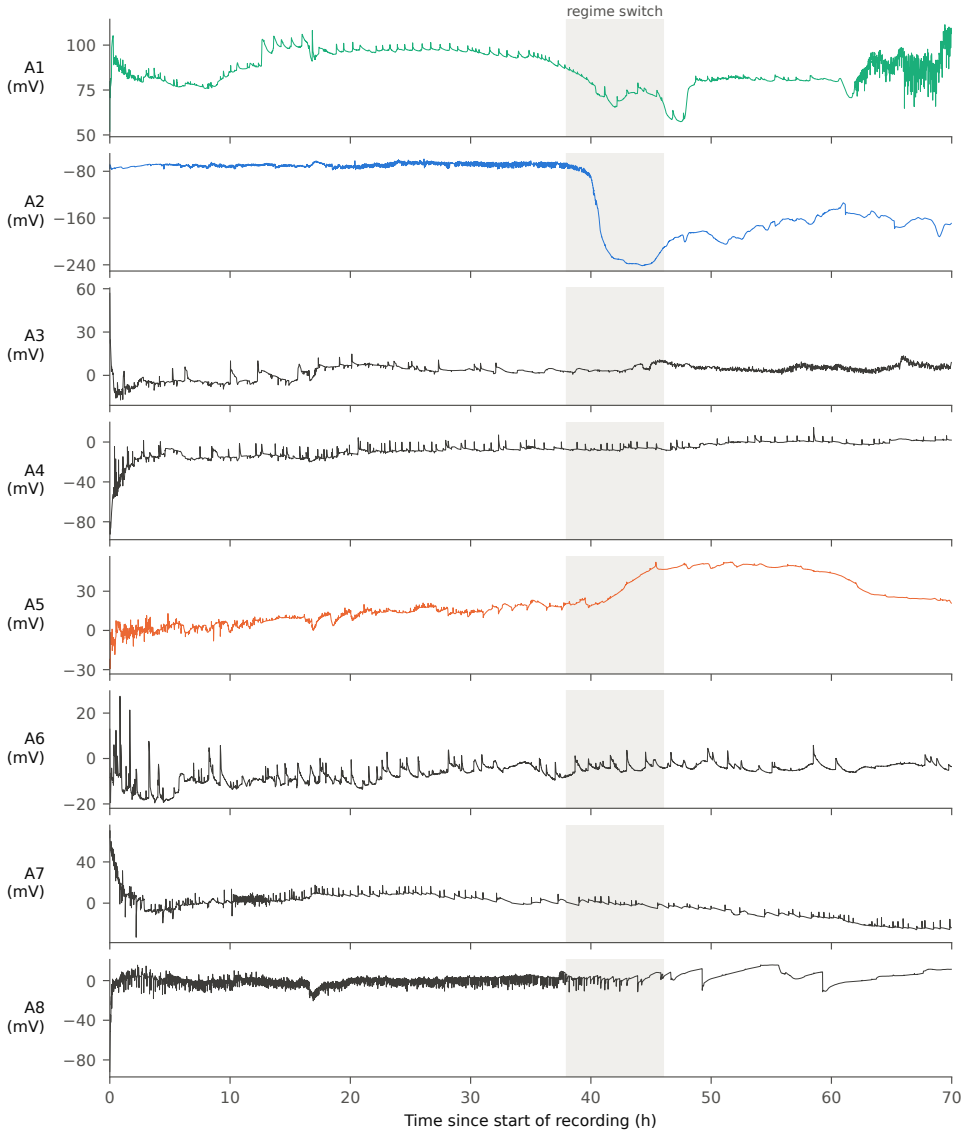


Fig. 3 Seventy hours of spontaneous electrical activity in recording A. Channels A1, A2 and A5, which take part in the regime switch analysed in Sect. 3.4, are drawn in colour, and the shaded band marks the switch (38–46 h). Traces are decimated tenfold for display.

Activity in recording A was not stationary. A2 was almost silent for the first four hours, then fired at 20 to 60 events per hour until 40 h, and afterwards fell silent for the remaining 30 h (Fig. 5a). A1 and A3 were active during the initial transient, quiescent through the middle of the record, and resumed firing late, A3 from about

42 h and A1 from about 62 h, when A1 entered a period of large irregular oscillations. A5 and A8 declined steadily and were nearly silent after 45 h, and A7 fell to a few events per hour.

Event polarity revealed a superficial form of inversion. On most channels, positive-going and negative-going excursions were comparable in number, but A8 produced 700 negative and 236 positive events, and its negative events were large (median −7.2 mV against +1.8 mV for positive ones), forming a train of sharp downward spikes that mirror the upward spikes of A4 and A7 (Fig. 4). A3 was also dominated by negative excursions (261 negative against 57 positive), though these were small step-like decrements rather than spikes. We return in the Discussion to why such sign inversion, although it superficially resembles negation, should not be counted as a NOT operation.

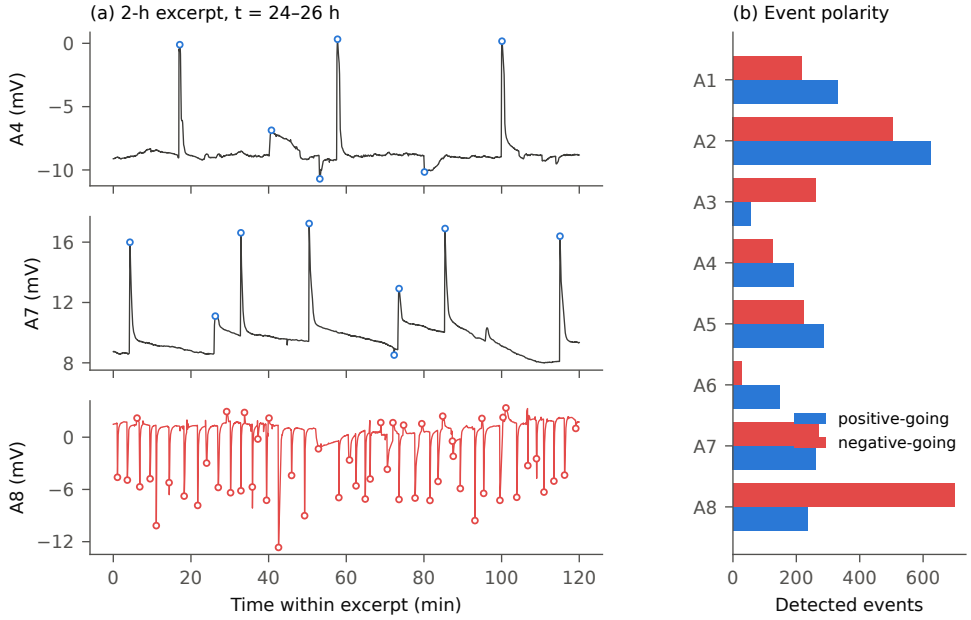


Fig. 4 Spike morphology and polarity in recording A. (a) Two hours of activity on A4, A7 and A8, with detected events marked by circles. A4 and A7 produce upward spikes with slow recovery, while A8 produces a dense train of downward spikes. (b) Number of positive-going and negative-going events detected on each channel over the full recording.

3.3 At the scale of spikes, the material copies

The most direct form of negation would be a spike on one channel that suppresses spikes on another. We found no evidence for it in either recording. In recording A, among the 56 directed pairs, 15 showed significant event-triggered facilitation at the nominal level of $p < 0.05$, with ratios R_{ij} between 1.21 and 2.18 (Fig. 5b). The

strongest effects ran from A6 and A7 to A1 and A3, and three pairs (A6 to A1, A6 to A3 and A7 to A3, each with $R_{ij} \geq 1.64$ and $p = 0.002$) remained significant after control of the false discovery rate at 5%, nine at 10%. The smallest ratio observed was 0.75, from A4 to A7, and it was not significant ($p = 0.08$). In recording B only three pairs reached nominal significance, all of them facilitatory (B5 to B8, $R = 1.16$; B8 to B5, $R = 1.12$; B8 to B7, $R = 1.84$), none survived correction, and again no pair showed significant suppression. Recording C was much quieter, with 292 events in 48 h, between 6 on C1 and 103 on C3, so that only 42 directed pairs could be tested. Two reached nominal significance, both facilitatory and both between C3 and C5 (C5 to C3, $R = 1.40$, $p = 0.002$, significant at a false discovery rate of 10%; C3 to C5, $R = 1.25$, $p = 0.022$), and no pair showed suppression. As shown in Sect. 3.8, these two channels move in opposite directions on the scale of an hour. Excitations therefore propagate between sites as positive copies of one another, a relation that is logically a BUFFER.

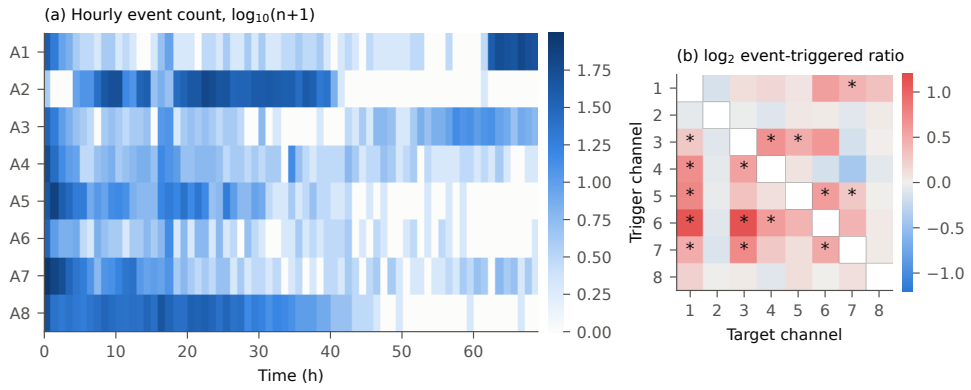


Fig. 5 Activity in recording A is partitioned in time but coupled positively at short lags. (a) Hourly event counts. A2 fires between 4 and 40 h and is silent thereafter, while A1 and A3 resume firing after the switch. (b) Directed event-triggered ratio R_{ij} on a logarithmic colour scale for 120-s windows, computed after excluding the first 3 h. Red indicates facilitation and blue suppression. Asterisks mark pairs with $p < 0.05$ against a ±30-min jitter null.

Within channels, the picture was similar with one exception. A2 showed self-facilitation (events in the 30–300 s window after an event were 7% more frequent than under jitter, $z = 5.0$), consistent with bursting. A8 showed the opposite: after each event, further events were 11% less frequent than expected ($z = -6.3$). This post-event refractoriness is the only fast suppressive relation between spikes we detected, and it is a channel suppressing itself rather than another.

3.4 At the scale of regimes, the material inverts

Between 38 and 46 h recording A underwent a reorganisation that involved three channels in different ways (Figs. 3 and 6a). A2, which had held a stable potential

near −68.6 mV while firing for 36 h, collapsed to below −230 mV and settled near −192 mV, crossing the midpoint of its transition at 40.42 h. At the same moment its spiking ceased. A1 declined in parallel with A2, beginning slightly earlier and crossing its own midpoint at 40.39 h; it then rebounded after 48 h and settled about 13 mV below its earlier level. A5 moved the other way. Its potential, which had drifted slowly upwards for 38 h, rose by 31.6 mV to a plateau near 50 mV, crossing its midpoint at 42.81 h, 2.39 h after the input.

Lagged correlation made the ordering explicit (Fig. 6b). The correlation between A2 and A5 was negative at every lag tested and reached its extreme, $r = -0.94$, when A5 was delayed by 2.85 h. The correlation between A2 and A1 was positive at every lag and peaked at $r = 0.78$ with A1 leading by 0.85 h. A single event in A2 was thus accompanied by a same-sign change on one side and an opposite-sign change, delayed by hours, on the other.

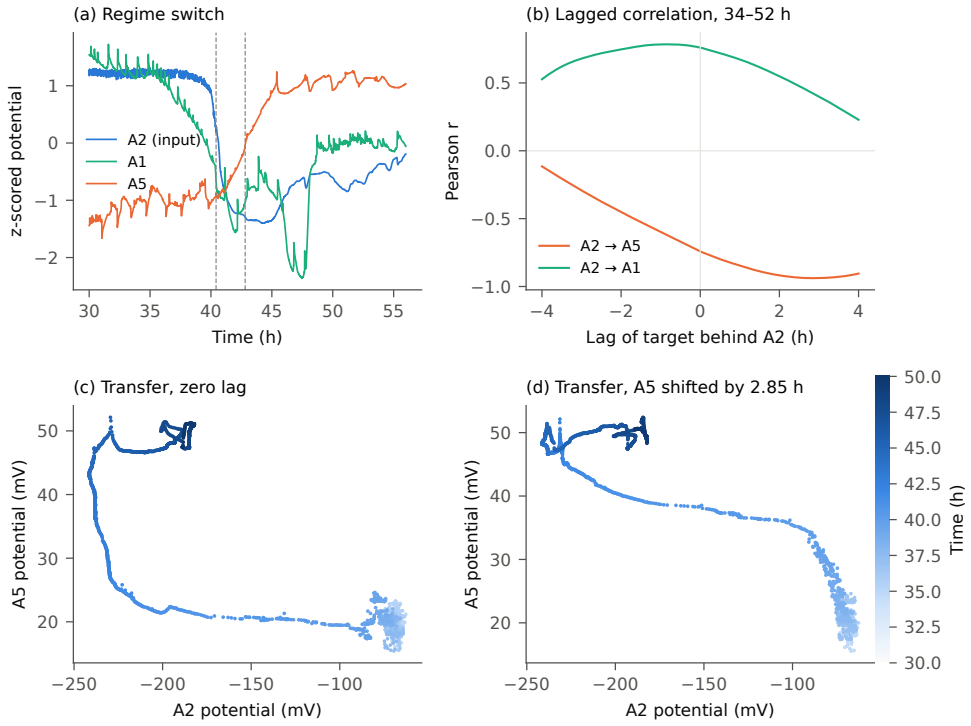


Fig. 6 In recording A a single change produces a copying and an inverting response. (a) z-scored 10-s averages of A2, A1 and A5 between 30 and 56 h. Dashed lines mark the half-transition times of A2 (40.42 h) and A5 (42.81 h). (b) Pearson correlation between A2 and each output as a function of the lag of the output, computed over 34–52 h. (c) Transfer relation between A2 and A5 at zero lag, coloured by time. (d) The same relation after shifting A5 back by 2.85 h, the lag of maximal anticorrelation.

The transfer relation from A2 to A5 had the shape of an inverter. At zero lag (Fig. 6c), A5 remained near 20 mV while A2 fell from −70 to about −180 mV, and then rose steeply to above 45 mV while A2 changed by only a few tens of millivolts more, the characteristic flat-steep-flat profile of a thresholded inverting switch. Part of this steepness is a consequence of the delay, because A2 had largely completed its fall before A5 had begun its rise. When the delay was removed (Fig. 6d), the relation became a graded, monotonically decreasing curve with Spearman correlation $\rho = -0.71$. The appropriate description is therefore that of a slow inverting relation whose output integrates the input over hours, rather than an instantaneous high-gain switch.

Binarisation converts these observations into truth tables (Table 1). When A2 was low, A5 was high in all 177 bins, and when A2 was high, A5 was low in 201 of 224 bins, giving $F_{\mathrm{NOT}} = 0.943$. None of 2,000 circularly shifted surrogates reached this value. The same input produced the opposite table on A1, which was dominated by agreement ($F_{\mathrm{BUF}} = 0.751$). A7 copied the input still more faithfully ($F_{\mathrm{BUF}} = 0.895$), as a consequence of its slow decline over the record.

Table 1 Truth tables relating the binarised potential of A2 (input X) to A5 and to A1 (outputs Y), counted in 10-min bins after the first 3 h of recording A ($N = 401$). Each cell gives the number of bins with the indicated combination of states.

	Output A5		Output A1	
Input A2	$Y = 0$	$Y = 1$	$Y = 0$	$Y = 1$
$X = 0$ (low, after switch)	0	177	139	38
$X = 1$ (high, before switch)	201	23	62	162
F_{NOT}	0.943		0.249	
F_{BUF}	0.057		0.751	
p (NOT, circular shift)	< 0.0005		0.96	

The truth-table test alone is not specific. A4 and A6 also gave F_{NOT} of 0.85 and 0.76, and both values were significant against the circular-shift null, because these channels drifted slowly upwards across the whole recording while A2 fell. The transition locality index separated the two situations. A5 concentrated 66% of its total excursion in the window of the switch, comparable to the input itself (−0.75), whereas the corresponding values were 0.29 for A4, 0.06 for A6, 0.15 for A3 and 0.24 for A8. A1 concentrated −0.44 of its excursion, with the same sign as the input. Only A5 thus combines a high NOT fidelity with a response that is localised in time to the input event.

3.5 Negation is expressed when the input moves

The sliding-window analysis shows when the inverting relation became visible (Fig. 7). For most of recording A, the 6-h Spearman correlation between A2 and A5 wandered between about −0.5 and +0.8 without consistent sign, because during quiescent periods the small fluctuations of the two channels were essentially unrelated. As the input

began to move, the correlation turned sharply negative, passing −0.73 in the window centred at 39.0 h and reaching −0.92 at 42.0 h, while the correlation with A1 rose to 0.97 at 39.5 h. Both relations decayed again once A2 had settled. The inverting relation is therefore not a fixed wiring diagram but a dependency that becomes observable when, and only when, the input carries a change.

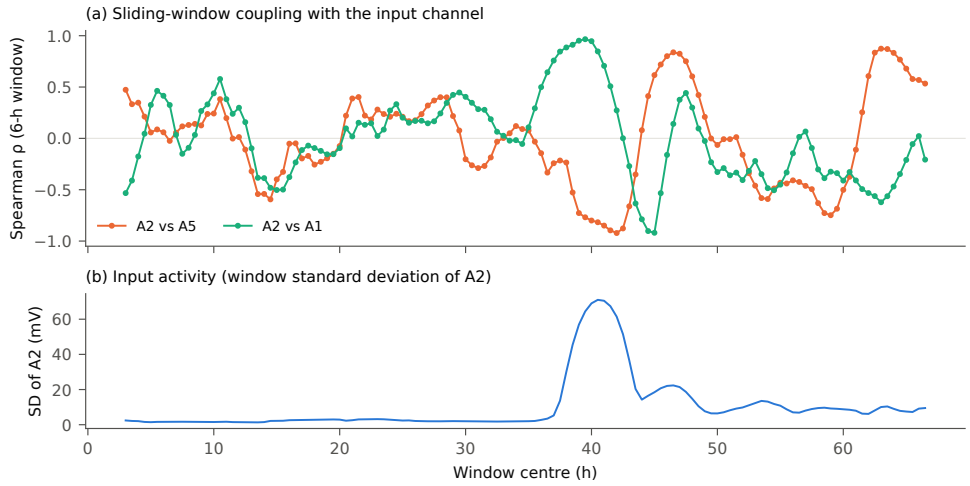


Fig. 7 When negation becomes observable in recording A. (a) Spearman correlation between A2 and A5 and between A2 and A1 in 6-h windows advanced in 30-min steps. (b) Standard deviation of A2 in the same windows, a measure of how much the input is changing. The strong anticorrelation with A5 coincides with the period of maximal input activity.

A second, independent form of inversion concerned not potentials but firing. Over hours 3 to 69, hourly event counts on A2 and A3 were negatively rank-correlated ($\rho = -0.46$), and the binarised activity of A3 was the negation of that of A2 in 75.8% of hours ($p = 0.018$ against 5,000 circular shifts). A3 was quiet throughout the 36 h in which A2 fired, and became active as A2 fell silent. No comparable partition was found between A2 and A1 ($F_{\mathrm{NOT}} = 0.49$, $p = 0.62$) or A7 ($F_{\mathrm{NOT}} = 0.44$, $p = 0.57$). A5 and A8, by contrast, copied A2 in their firing ($\rho = 0.71$ and 0.80), so that A5 copied the input in its spike rate while inverting it in its potential, a dual representation in a single site to which we return below.

3.6 An independent sample repeats the complementary split

Recording B, made seven months earlier on a separately prepared sample, also contained a slow regime switch late in the record, between about 36 and 44 h (Fig. 8). Its structure was the same in kind as in recording A, although the identity of the leading site and its direction differed. Six of the eight channels changed substantially across the switch, and they split into two groups that moved in opposite directions. B1, B3

and B5 rose, by 59.8, 45.5 and 14.8 mV, with transition locality indices of 0.55, 0.42 and 0.44, while B2, B6 and B7 fell, by 49.6, 29.4 and 24.2 mV, with indices of −0.64, −0.75 and −0.74. B4 and B8 changed little (−0.18 and −0.03).

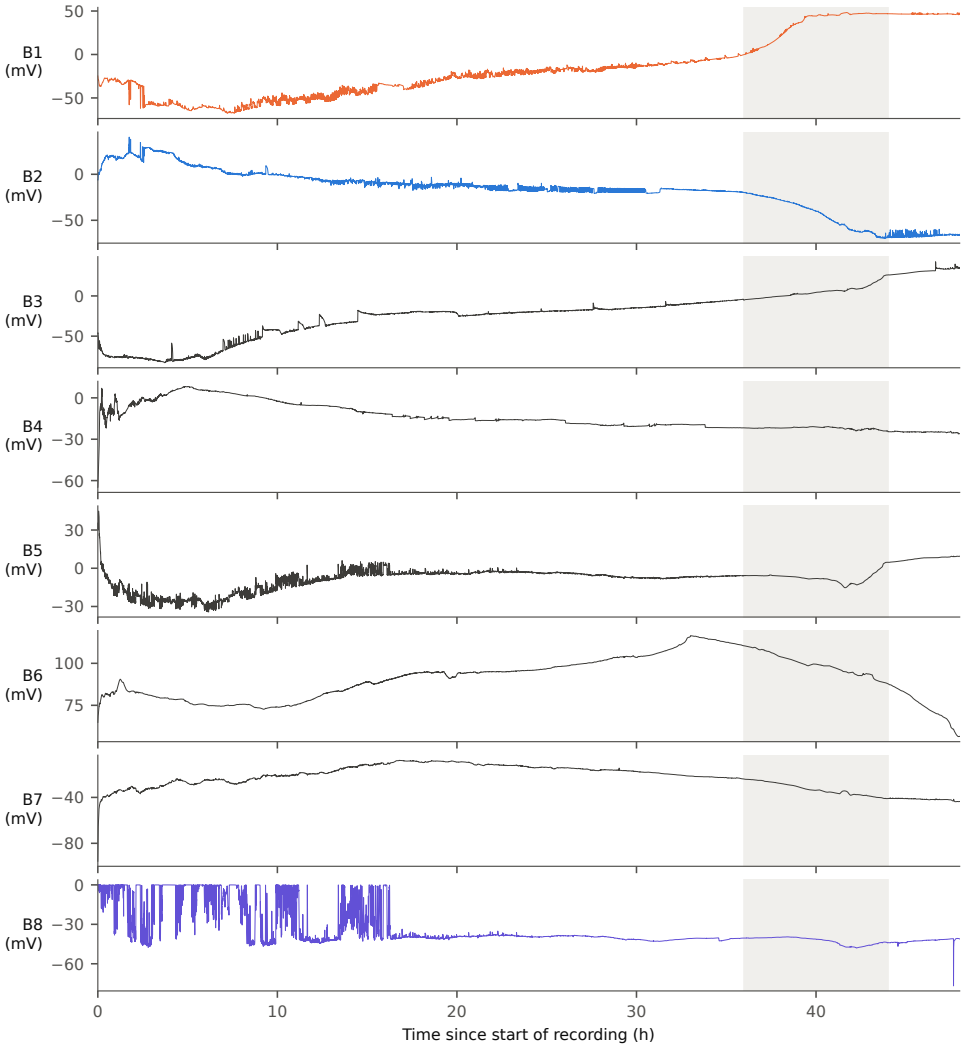


Fig. 8 Forty-eight hours of spontaneous electrical activity in recording B, from an independently prepared Glu–Phe–Asp sample. B1 and B2, the leading rising and falling channels of the regime switch, and B8, which toggles between two discrete levels during the first 16 h, are drawn in colour. The shaded band marks the switch (36–44 h). Traces are decimated fivefold for display.

The switch unfolded as an ordered cascade (Fig. 9a). B1 crossed its midpoint first, at 37.76 h, followed by B7 falling at 38.69 h, B2 falling at 40.25 h, B3 rising at 41.79 h, and B6 falling and B5 rising at 43.49 and 43.66 h. Taking B1 as the leading channel, the correlations with the falling channels were negative at every lag and nearly perfect at their optimum, $r = -0.995$ for B2 delayed by 2.57 h and $r = -0.981$ for B7 delayed by 1.57 h, whereas the rising B3 was positively correlated with B1 ($r = 0.97$ at a delay of at least 4 h, the edge of the range tested; Fig. 9b). In recording A the leader fell and its inverted partner rose 2.4 h later; in recording B the leader rose and its inverted partner fell 2.6 h later. The delay of the inverting response was thus similar in the two samples, while its sign was reversed, as expected if the relation is symmetric and only the timing assigns the roles of input and output.

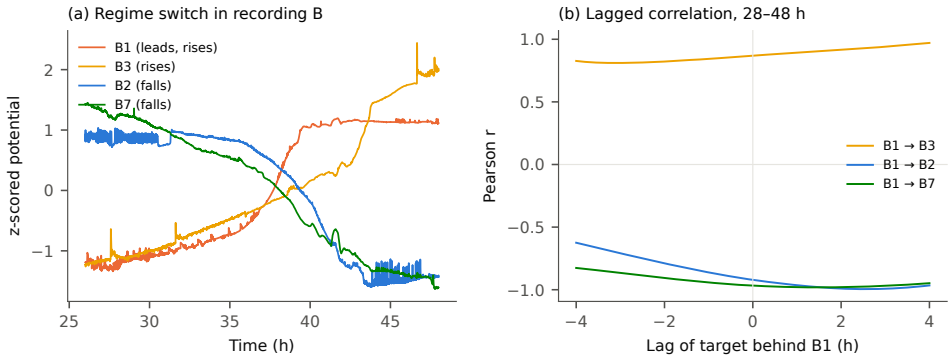


Fig. 9 The regime switch of recording B. (a) z-scored 10-s averages of the leading channel B1, the co-rising channel B3 and the counter-moving channels B2 and B7 between 26 and 48 h. (b) Pearson correlation between B1 and each of these channels as a function of the lag of the target, computed over 28–48 h.

Table 2 Truth tables relating the binarised potential of B1 (input X) to B2 and to B3 (outputs Y), counted in 10-min bins after the first 3 h of recording B ($N = 270$). The input is high only after the switch, so the two rows are unequal in size.

	Output B2		Output B3	
Input B1	$Y = 0$	$Y = 1$	$Y = 0$	$Y = 1$
$X = 0$ (low, before switch)	74	135	135	74
$X = 1$ (high, after switch)	61	0	0	61
F_{NOT}	0.726		0.274	
F_{BUF}	0.274		0.726	
p (circular shift)	< 0.0005 (NOT)		0.20 (BUFFER)	

The truth tables of recording B are less balanced than those of recording A because the leading channel spent only the last 10 h of the record in its high state (Table 2).

Within that period, however, the relation was exact. In all 61 bins in which B1 was high, B2 was low, and in all 61 of them B3 was high. Over the whole record, B2 was the negation of B1 in 72.6% of bins ($p < 0.0005$), and B7 showed the same table ($F_{\mathrm{NOT}} = 0.726$, $p = 0.005$). The co-rising B3 had the mirror table, with $F_{\mathrm{BUF}} = 0.726$, but this agreement was not significant against the circular-shift null ($p = 0.20$), because both B1 and B3 rose gradually through most of the record and shifted copies of such ramps agree with each other by chance. Taken together, recordings A and B show that a slow switch in a proteinoid ensemble partitions the electrode sites into two complementary sets, each of which carries the negation of the other.

3.7 A bistable site and its copying and inverting partners

Recording B contained a second phenomenon not seen in recording A. During its first 16 h, B8 did not spike but toggled between two discrete levels, an upper level close to 0 mV and a lower level near −45 mV, spending 56% of the time between 3 and 16 h in the upper state (Fig. 10a). After the first 3 h, 199 switches were detected (99 up and 100 down), the last at 16.25 h, after which the channel remained in the lower state. Each switch is a discrete binary event with a known sign, which makes it possible to ask directly how other sites respond to a change of state.

The answer was again twofold (Fig. 10b,c). B5 stepped in the same direction as B8 at 91.5% of switches, with a median signed step of +3.52 mV, and B6 did so at 68.8% (+0.04 mV); both agreements were significant against random times ($p < 0.0005$). B7 stepped in the opposite direction at 68.8% of switches (median signed step −0.15 mV, $p < 0.0005$), and B4 and B3 did so at 63.3% and 62.3% ($p < 0.0005$ in both cases), with B1 weaker but still significant (58.3%, $p = 0.011$). B2 was unrelated (50.3%). The switch-locked median traces show that the copying response of B5 is a sharp step coincident with the switch, while the inverting response of B7 develops over the following tens of seconds (Fig. 10b). A single binary change of state at one site was therefore expressed as a copy at some neighbouring sites and as its negation at others, within a minute.

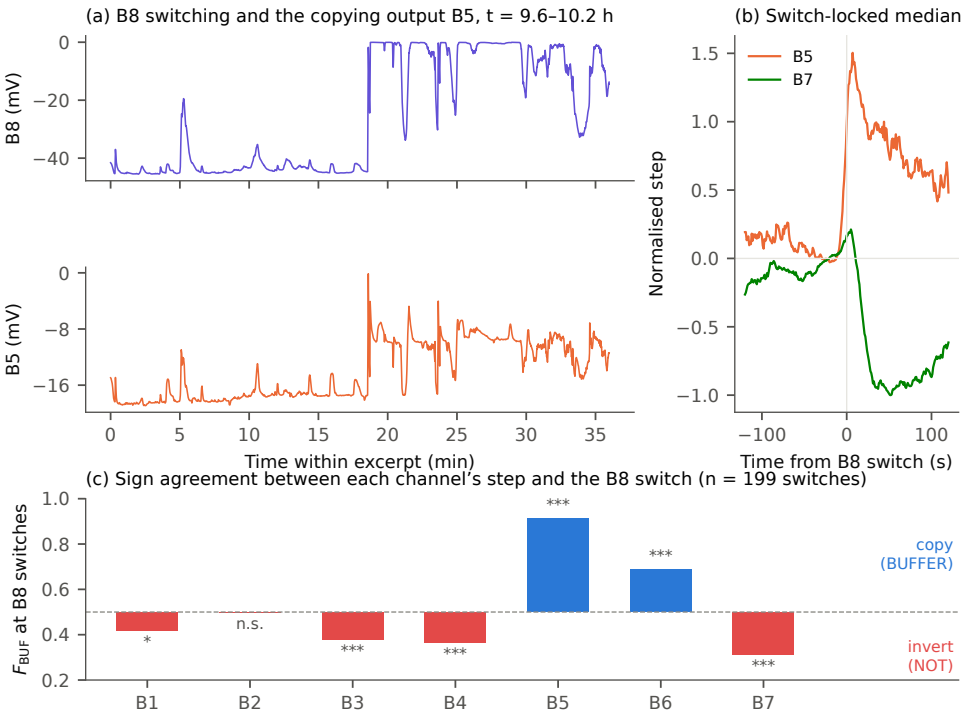


Fig. 10 A bistable site in recording B has copying and inverting partners. (a) Ten minutes of B8 switching between its upper and lower levels, and the simultaneous steps of B5. (b) Median of the B5 and B7 traces aligned on B8 switches, with down switches sign-inverted and pooled with up switches, each normalised to its largest absolute value after the switch. (c) Fraction of the 199 switches at which each channel stepped in the same direction as B8. Bars above 0.5 indicate copying, bars below 0.5 inversion. Asterisks give the significance against random times with permuted signs (*, $p < 0.05$; ***, $p < 0.001$; n.s., not significant).

3.8 A third sample: solitary pulses with copying and inverting partners

Recording C, made on 20 March 2025 from a third, independently prepared sample, had no regime switch and no bistable site. Its slow dynamics were instead punctuated by solitary pulses lasting tens of minutes (Fig. 11a). Five pulses of C1 exceeded the detection threshold, at 10.1, 19.4, 20.5, 24.1 and 25.6 h. Four were positive and one negative, and their amplitudes in the detrended signal were 4.5 to 6.4 mV. The question is the same as for the switches of B8: when one site changes, how do the others respond?

Every pulse was carried by three other sites, two with its sign and one against it (Fig. 11b,c). C4 and C5 moved with C1 at all five pulses, with correlations of 0.74 to 0.99 and signed amplitudes of 4.0 to 6.7 mV and 3.4 to 4.9 mV. C3 moved against C1 at all five, including the negative pulse, with correlations of −0.72 to −0.91 and signed amplitudes of −1.5 to −3.6 mV. The responses followed C1 within minutes,

with median lags of the maximal absolute correlation of 2 min for C4, 3 min for C5 and 4 min for C3. Against random times, the inversion was specific to the pulses ($F_{\mathrm{NOT}} = 1$, $p = 0.018$), whereas the copies were not ($p = 0.38$ for C4 and $p = 0.77$ for C5), because C4 and C5 were positively correlated with C1 at most moments of the recording. In this sample, then, copying is a standing relation, while negation appears only when the input carries a pulse, as it did at the regime switch of recording A (Sect. 3.5). C8 also agreed with C1 more often than at random times ($F_{\mathrm{BUF}} = 1$, $p = 0.039$), but with weaker correlations of 0.19 to 0.77, and C2, C6 and C7 showed no consistent relation.

The pair C3–C5 links this result to the analysis of spikes. At the scale of seconds, spikes on C3 and C5 facilitated each other (Sect. 3.3); at the scale of an hour, their potentials moved in opposite directions at every pulse. The same two sites therefore copy at one time scale and invert at another.

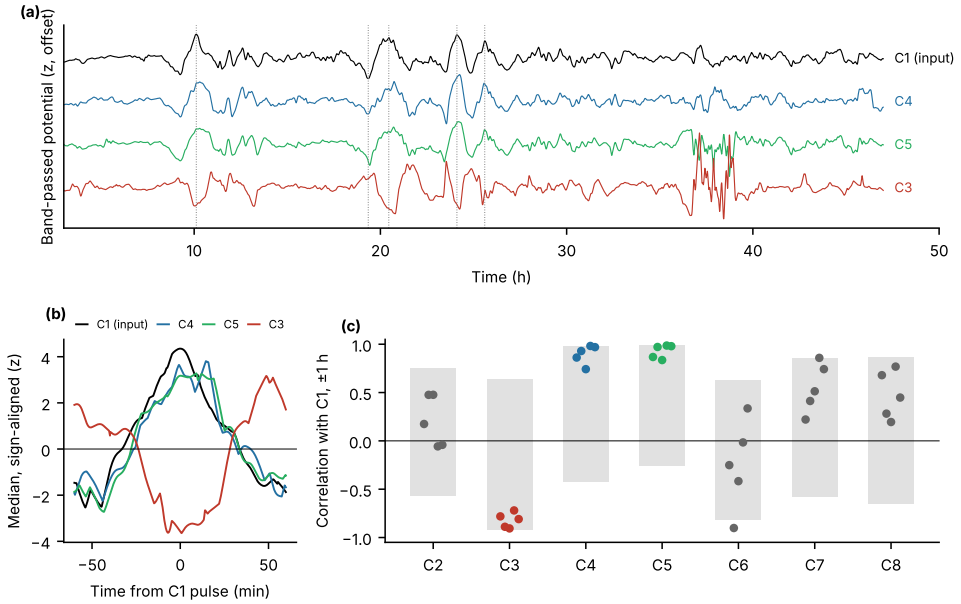


Fig. 11 Solitary pulses in recording C, from a third independent sample, have copying and inverting partners. (a) Band-passed (10 min to 4 h), robustly z-scored signals of C1, C4, C5 and C3 between 3 and 47 h, offset for clarity. Dotted lines mark the five pulses detected on C1. (b) Median responses aligned on the C1 pulses, with the negative pulse sign-inverted. (c) Correlation between C1 and each channel in a ±1-h window around each pulse (dots), and the 2.5–97.5% range of the same correlation at random times (grey bars).

3.9 An imposed input is copied, not inverted

In recording D, light was switched on and off at 30 min intervals on two days (Fig. 12a). D1 responded in all 18 cycles, with a median rise of 1.50 mV within 5 min of onset. Its

potential continued to rise during illumination and fell after offset. D8 showed onset steps of +0.26 mV in all 18 cycles and offset steps of −0.18 mV in 17 of 18 cycles. D5 rose by 0.06 mV at every onset and fell by 0.05 mV at every offset. Its potential relaxed towards baseline during illumination (Fig. 12e). D3 rose by 0.02 mV at every onset. D4 rose by 0.27 mV in 16 of 18 cycles. All five responses were significant against random times within the same days ($p \leq 0.008$). No responsive channel showed an inverse response. D7 was the only channel with a consistent opposite sign. It shifted by −0.4 μV at 17 of 18 onsets. However, its potential remained within a few microvolts of zero throughout the recording. This sub-microvolt shift on an otherwise inactive input is more plausibly attributed to electrical pickup during switching than to a material response. Thus, the ensemble behaved as a set of buffers with different gains and time courses. No copying–inverting pair was identified under the imposed input.

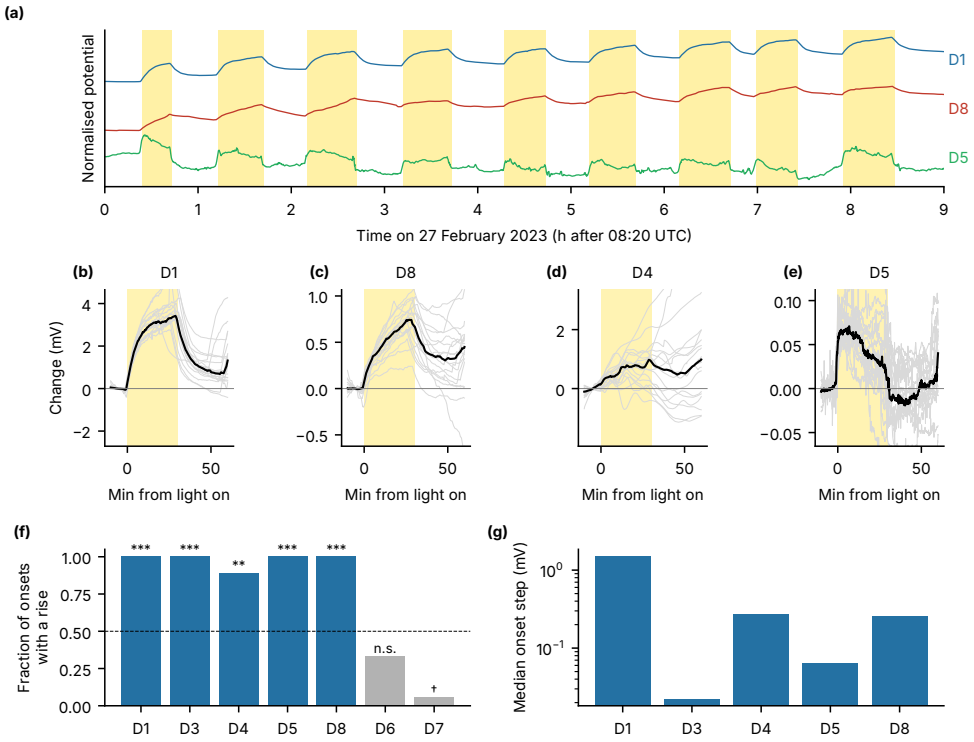


Fig. 12 An imposed light input is copied by every responsive site in recording D. (a) Potentials of D1, D8 and D5 on 27 February 2023, smoothed over 1 min, normalised and offset. Shaded bands indicate the 30 min illuminated periods. (b–e) Responses of D1, D8, D4 and D5 aligned to the 18 light onsets. Grey traces show individual responses, and black curves show their medians. The shaded band indicates the illuminated period. (f) Fraction of onsets at which each channel rose (***, $p < 0.001$; **, $p < 0.01$; n.s., not significant against random times). D6 and D7 (grey) were non-functional inputs. The opposite sign of D7 (†) reflects a sub-microvolt shift attributed to electrical pickup. (g) Median potential step at light onset.

3.10 A fast periodic input is distributed with site-specific phases

In recording E, every site responded to the nominal 10 Hz flicker in every session (Fig. 13a,b). The light-locked line exceeded the neighbouring spectrum, with median signal-to-noise ratios of 12–64 in 10 min windows. Harmonics were visible up to the fourth, indicating a pulse-like response consistent with on–off illumination. Observed amplitudes spanned two orders of magnitude, from 1–4 μV on E4 to 117–284 μV on E2 (Fig. 13d). Site rankings were identical across sessions. Phases relative to E2 were stable within sessions, with mean resultant lengths of at least 0.97. They also varied little across the five sessions and four colours, with circular standard deviations of 4°–16° (Fig. 13c). E3 and E5 followed E2 within 15°. The relative phases of E1, E8, E6 and E4 were +34°, −48°, +125° and −117°, respectively. E7 had the second-largest response (90–146 μV) and was nearly in anti-phase with E2, at $(168 \pm 13)°$. Thus, the same periodic input produced responses both aligned with and opposed to E2. Without a light sensor, however, we cannot determine whether E2 or E7 follows the light directly. Only their relative opposition is established. Moreover, phases extended across the full circle rather than being confined to 0° and 180°. This distribution is consistent with differences in both delay and response sign. Anti-phase between differential channels can also arise from electrode-pair orientation relative to a common source. This is the linear sign inversion discussed for spikes in Sect. 4.2. In recording D, however, slowly switched illumination produced no opposite responses. Orientation alone therefore did not generate opposite responses in that sample. For recording E, these data cannot distinguish a geometric origin of E7's anti-phase from a material response with the opposite sign at the scale of an individual flash.

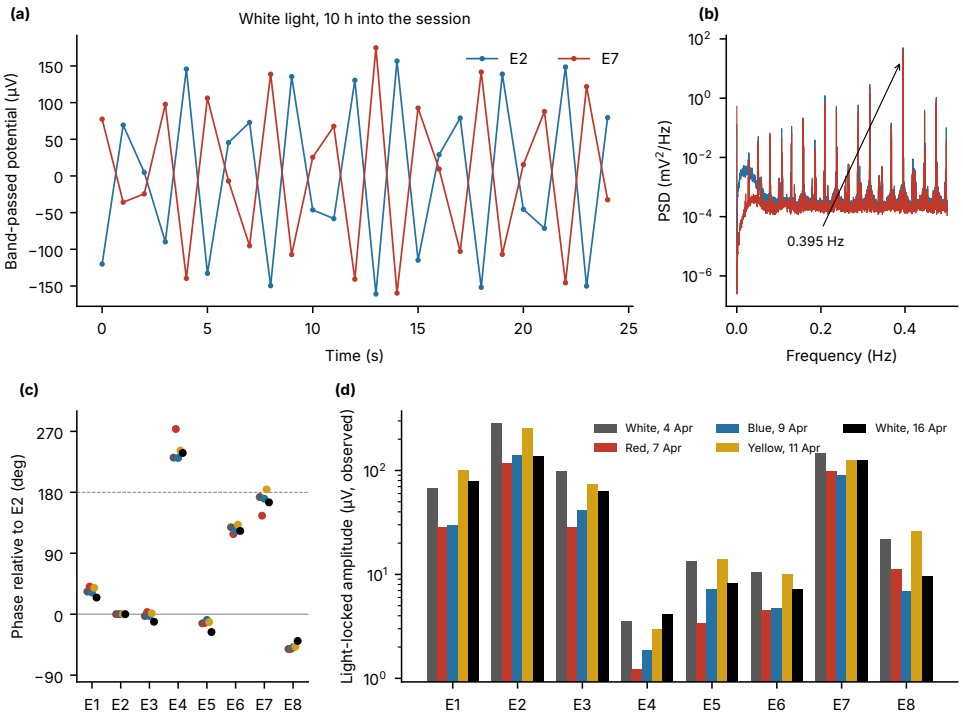


Fig. 13 Proteinoids respond to light flickering at a nominal 10 Hz with site-specific phases (recording E). (a) A 25 s segment of the band-pass-filtered (0.30–0.49 Hz) potentials of E2 and E7 after 10 h under white light. The 0.395 Hz alias appears in anti-phase at the two sites. (b) Power spectral densities of E2 and E7, showing the light-locked line at 0.395 Hz and its harmonics. (c) Phase of each site relative to E2 across the five sessions (white, 4 April; red, 7 April; blue, 9 April; yellow, 11 April; white, 16 April). The dashed line indicates anti-phase. (d) Observed amplitude of the light-locked oscillation at each site and session.

4 Discussion

4.1 Where negation lives in a proteinoid ensemble

The intuitive place to search for chemical negation is at the level of the spike, with one excitation inhibiting another. Our data argue against that picture for this material. In all three recordings, fast interactions between spikes were uniformly facilitatory, consistent with excitation spreading through the suspension by shared ionic currents or by contact between microspheres. A medium in which every fast interaction between excitations is positive behaves, logically, as a network of buffers and OR-like junctions. It can relay a signal and it can merge signals, but it cannot invert one.

Negation appeared at two different levels of organisation. The first is the slow redistribution of potential among regions of the ensemble. When one region underwent a large, abrupt shift, another region responded hours later with a shift of the opposite

sign, while a third moved with the first. The second is the discrete switching or solitary pulsing of a single site, at which neighbouring sites moved either with it or against it within a minute (B8) or within a few minutes (C1). The simplest physical reading of both is conservative, in the sense that charge, ions or protonation states lost from one region accumulate in another. The micrographs make this plausible. The material is a dense population of compartments that bud, fuse and deform (Fig. 2), and proteinoids are rich in carboxylate side chains from glutamic and aspartic acid and in hydrophobic phenylalanine residues. A reorganisation of microsphere aggregates, the opening or fusion of compartments, a change in local pH, or a redistribution of counterions would all be expected to raise the potential in one place as they lower it elsewhere. A constraint of this kind, $\Delta V_A \approx -\kappa\,\Delta V_B$ with $\kappa > 0$, is an inverting relation that requires no design. It is a consequence of conservation in a spatially extended medium, and the delay of hours seen in recordings A and B is what one expects if the coupling is diffusive rather than electrical.

This reading suggests that inversion represents a thermodynamically and energetically accessible phenomenon in abiotic media. Copying requires the input to drive the output in its own direction, which in a chemical medium means an excitation that propagates. Inverting requires only that the input and output compete for a shared, limited resource. Competition for a common pool is among the most generic relations in any chemical system, and it is plausible that prebiotic matter 'discovered' inversion long before it discovered the reliable propagation of spikes, simply because conservation laws impose it.

4.2 Trivial and functional negation

Several relations in our data look like negation but should be distinguished from it. The first is the dominance of negative spikes on A8. In a differential recording the sign of a spike depends on which electrode of the pair is closer to its source, so an identical excitation read by a pair with reversed geometry would appear inverted. Such sign inversion is a linear map of the form $y = -x$ with no threshold and no state, and it is undone by relabelling the electrodes. It is negation only in the sense that a voltmeter connected backwards is a NOT gate. A8 is nevertheless interesting for a different reason, since it was the only channel to display refractoriness, so that its own past firing suppresses its immediate future. Self-inhibition of this kind is the elementary ingredient of relaxation oscillators and, when chained, of ring oscillators built from inverters Elowitz and Leibler (2000).

The second is agreement in binarised truth tables that arises from slow monotonic drift. A4 and A6 passed the truth-table test merely because they drifted upward while the input drifted downward, and the co-rising B3 in recording B agreed with B1 for the same reason without reaching significance. A naive search for logic gates in long recordings will always find such pairs. We regard the combination of high truth-table fidelity, temporal locality of the output change, and a consistent lag as a minimal set of criteria for calling a relation functional negation in unstimulated recordings. The relations A2–A5, B1–B2 and B1–B7 met all three. For discrete events, such as the switches of B8 and the pulses of C1, the corresponding test is agreement at the events compared with agreement at random times, which B7 and C3 passed.

The third concerns the bistable site B8. Its upper level lay within a fraction of a millivolt of zero, which is also the reading a differential input gives when its two electrodes are shorted together, for example by a conductive bridge of material, or when both lose contact with the medium. The switching of B8 may therefore reflect the intermittent formation and rupture of a physical connection rather than a change of chemical state. This does not remove the interest of the observation, because the consequence for the rest of the ensemble, a copy at one set of sites and an inversion at another, is exactly what the conservation argument above predicts for any local change of current path. It does mean that B8 should be regarded as a naturally occurring switch in the medium rather than as a demonstration that a single microsphere has two stable states.

4.3 One input, two outputs: a chemical dual rail

The most consequential observation may be that each change did not drive one output but two, of opposite sign. In digital engineering, dual-rail encoding represents each logical variable by a pair of wires carrying x and $\bar{x}$. Once both polarities of every variable are available, any Boolean function can be built from monotone gates alone, because every literal of a disjunctive normal form is already present. The A2 event produced exactly such a pair, with A1 carrying a copy of the input and A5 carrying its negation. The B1 event produced the same arrangement with B3 as the copy and B2 and B7 as negations, and the B8 switches did so on a time scale of seconds, with B5 as the copy and B7 as the principal negation. In recording C, each pulse of C1 was copied by C4 and C5 and negated by C3. Every one of the three independent samples thus produced at least one dual-rail pair. Figure 14 summarises these arrangements.

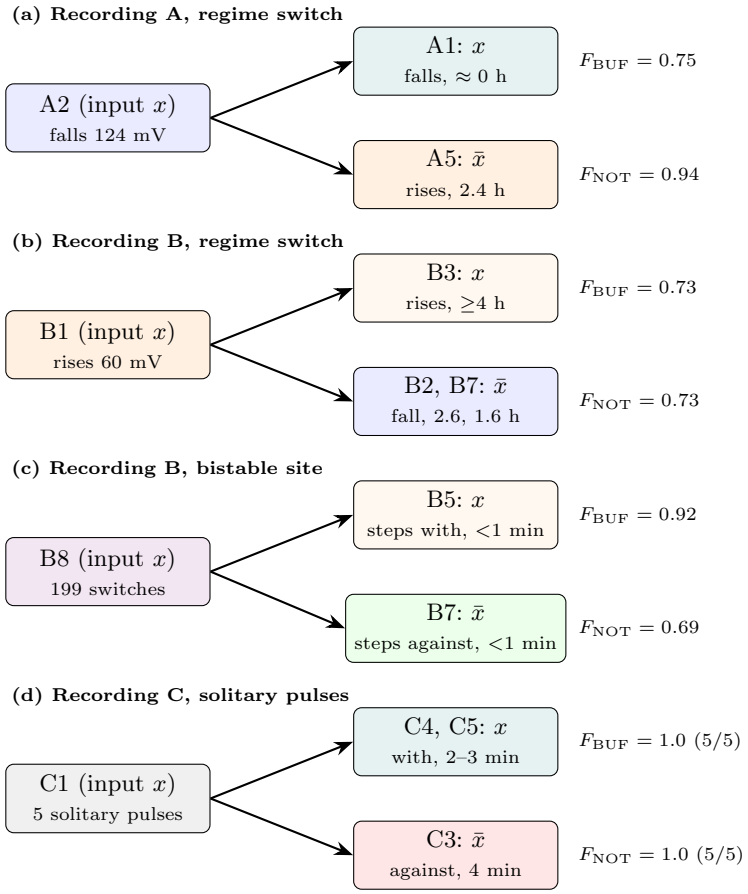


Fig. 14 Schematic of the dual-rail relations observed in the three recordings. In each case one change is expressed as a same-sign change at one site (x) and as an opposite-sign change at another ($\bar{x}$). Times give the delay of each output relative to the input. Fidelities are from Tables 1 and 2 for the regime switches from the sign agreement at B8 switches for the bistable site, and from the sign of the correlation at C1 pulses for the solitary pulses.

A5 also carried a dual representation on its own, copying A2 in its firing rate while inverting it in its potential. A single region of the material thus held x in one physical variable and $\bar{x}$ in another. In living cells, similar multiplexing is common when the activity and the abundance of a molecular species report different aspects of the same signal Bray (1995). In a protocell-like material it suggests that the choice of which variable to read, spikes or potential, already determines whether the material is seen to copy or to invert.

4.4 Spontaneous inversion, driven copying

Recording D distinguishes spontaneous changes from responses to imposed illumination. During spontaneous activity, a change at one site was accompanied by copying

at some sites and inversion at others. Under slowly switched illumination of the whole suspension, all responsive sites moved in the same direction. Their amplitudes and time courses differed. This pattern is consistent with the proposed conservation mechanism. Internal redistribution can produce opposite signs when gains in some compartments are balanced by losses elsewhere. Illumination of the whole suspension could instead drive a common response through thermal or photochemical changes. In recording D, inversion was therefore associated with internally generated change, whereas the imposed illumination produced copying. Using this behaviour as a gate may require a local input that initiates redistribution and generates an inverted response elsewhere. This prediction could be tested with a voltage step at one electrode pair or illumination of a limited region. The fast periodic input in recording E provides a further qualification. Under nominal 10 Hz flicker, sites showed reproducible relative phase differences. E7 remained nearly in anti-phase with E2, the strongest responder, in every session. The origin of this opposition remains unresolved, so it cannot establish material inversion. Nevertheless, the result shows that a fast input reaching the whole suspension can produce different phases at different sites. Together, these observations suggest that both the spatial extent and timescale of an input may influence whether sites respond in phase.

4.5 Implications for the origin of logic

If negation is a by-product of conservation and competition, the evolutionary problem is not how chemistry invented inversion but how it learned to use it. Four features of our observations bear on this. First, the inverting relation between regions was slow, with a delay of about 2.5 h in both samples, which sets a lower bound on the timescale over which any inference built on it could operate. Second, it was episodic, visible only when the input changed, which means that negation in such media is a property of events rather than of standing structure. Third, it coexisted with copying, so that the minimal resource for complete logic, the availability of both polarities of a variable, was present without any selection. Fourth, when a site changed state abruptly, as B8 did, or emitted a solitary pulse, as C1 did, the inverting response followed within minutes, showing that the same medium can express negation on time scales differing by two orders of magnitude depending on how sharply the input changes. Proteinoid ensembles have previously been shown to implement logic gates when stimulated Mougkogiannis and Adamatzky (2023b) and to change with experience Mougkogiannis and Adamatzky (2023a). The present results suggest that the raw material for such behaviour is present in their spontaneous dynamics, and that stimulation may select among relations that the material already forms rather than create them.

4.6 Limitations

The slow inverting relations rest on one regime switch in each of two samples, and the faster ones on 199 switches of one site and five pulses of another. The three samples showed different kinds of events, and recording C had no regime switch at all, so we cannot estimate how often each kind of event occurs or what triggers it. What recurred in all three was the response: a copy at some sites and an inversion at others.

The inversion in recording C rests on five pulses, and its significance against random times ($p = 0.018$) is correspondingly modest. No external input was applied in recordings A–C. The reported inversions therefore describe relations between spontaneously changing sites. They do not establish logic gates, which require controlled inputs and outputs that follow a prescribed logical rule for each input state. Recording D included an imposed input but used a single sample with only five functional channels. No light sensor was recorded, so light transitions were identified from D1 itself. Moreover, illumination reached the whole suspension rather than a single site. Recording E also lacked a light sensor, leaving the phase of the illumination unknown. Its colour sessions were performed sequentially on one sample. Colour effects therefore cannot be separated from ageing. Its anti-phase relation may also arise from electrode-pair orientation. The one recording with an imposed input, recording D, has its own limitations: it is a single sample, it has only five functional channels, no light sensor was recorded, so the transitions were located on D1 itself, and the light acted on the whole suspension rather than on one site. The direction of causation is inferred from temporal precedence and is compatible with a common hidden cause acting on several sites with different delays. The bistable site B8 may reflect an intermittent short or loss of contact rather than a chemical state, as discussed above. The micrographs were obtained from a separate aliquot of the same formulation after drying, and they describe the morphology of the material rather than of the particular population between the electrodes during recording. The physical mechanism we propose, conservative redistribution of charge among compartments, remains to be tested by simultaneous measurements of pH, conductivity and morphology. Finally, our criteria for functional negation were chosen to exclude artefacts identified in these data. A local input would directly test whether the spontaneous relations can be driven. For example, a voltage step at one electrode pair could test whether other pairs reproduce the observed split into copying and inverting responses.

5 Conclusion

Proteinoid microspheres made of glutamic acid, phenylalanine and aspartic acid, recorded without any stimulation in three independent samples, displayed both of the elementary relations from which logic is built. Fast interactions between spikes were positive and copied excitations from one region to another. Slow regime switches, by contrast, split the electrode sites into two complementary groups, so that a large shift at one site was followed hours later by a shift of opposite sign at another, matching the truth table of negation in up to 94% of observations, while a third site copied the same input. At a site that switched abruptly between two levels, and at a site that emitted solitary pulses, the same complementary split appeared within minutes, so that every sample produced at least one copying and one inverting partner of the same change. In this material inversion is not a property of a spike but of a constrained redistribution among compartments, and it appears in the company of its complement, as a dual rail. We suggest that prebiotic matter did not have to invent negation, because conservation and competition provided it, and that what remained to be discovered was how to make it fast. When an input was imposed, by switching a light on and

off over the whole suspension, every responsive site copied it and none inverted it. Inversion in this material is thus a property of its own redistributions, and whether it can be harnessed as a gate depends on finding an input that acts locally rather than everywhere at once. Switching illumination on and off over the whole suspension produced copying at every responsive site. None showed inversion. This pattern is consistent with inversion arising from internal redistribution. Using this behaviour as a gate would require a reproducible inverted response to a controlled local input.

Acknowledgements. Authors are grateful to David Paton for helping with SEM imaging.

Declarations

Funding. The research was supported by EPSRC Grant EP/W010887/1 "Computing with proteinoids"

Competing interests. The authors declare no competing interests.

Data availability. The raw PicoLog recordings (recording A, 7–10 September 2025; recording B, 16–18 February 2025; recording C, 20–22 March 2025; Glu–Phe–Asp pure formulation; recording D, 24 February–1 March 2023, light switched every 30 min; recording E, 4–18 April 2025, light flickering at 10 Hz); and the original SEM images are available from the corresponding author on reasonable request.

Author contribution. P.M. designed and performed the experiments, analysed the data and wrote the manuscript. A.A. conceived the study, supervised the work and revised the manuscript. Both authors approved the final version.

References

Adamatzky A (2019) A brief history of liquid computers. Philosophical Transactions of the Royal Society B 374(1774):20180372. https://doi.org/10.1098/rstb.2018.0372

Adamatzky A (2021) Towards proteinoid computers. Hypothesis paper. BioSystems 208:104480. https://doi.org/10.1016/j.biosystems.2021.104480

Adamatzky A, De Lacy Costello B, Asai T (2005) Reaction-Diffusion Computers. Elsevier, Amsterdam

Alon U (2007) Network motifs: theory and experimental approaches. Nature Reviews Genetics 8(6):450–461. https://doi.org/10.1038/nrg2102

Benjamini Y, Hochberg Y (1995) Controlling the false discovery rate: a practical and powerful approach to multiple testing. Journal of the Royal Statistical Society: Series B (Methodological) 57(1):289–300. https://doi.org/10.1111/j.2517-6161.1995.tb02031.x

Bray D (1995) Protein molecules as computational elements in living cells. Nature 376(6538):307–312. https://doi.org/10.1038/376307a0

Elowitz MB, Leibler S (2000) A synthetic oscillatory network of transcriptional regulators. Nature 403(6767):335–338. https://doi.org/10.1038/35002125

Fox SW (1988) The Emergence of Life: Darwinian Evolution from the Inside. Basic Books, New York

Fox SW, Harada K (1958) Thermal copolymerization of amino acids to a product resembling protein. Science 128(3333):1214. https://doi.org/10.1126/science.128.3333.1214

Gardner TS, Cantor CR, Collins JJ (2000) Construction of a genetic toggle switch in *escherichia coli*. Nature 403(6767):339–342. https://doi.org/10.1038/35002131

Grün S (2009) Data-driven significance estimation for precise spike correlation. Journal of Neurophysiology 101(3):1126–1140. https://doi.org/10.1152/jn.00093.2008

Hjelmfelt A, Weinberger ED, Ross J (1991) Chemical implementation of neural networks and Turing machines. Proceedings of the National Academy of Sciences USA 88(24):10983–10987. https://doi.org/10.1073/pnas.88.24.10983

Kauffman SA (1969) Metabolic stability and epigenesis in randomly constructed genetic nets. Journal of Theoretical Biology 22(3):437–467. https://doi.org/10.1016/0022-5193(69)90015-0

Mann S (2012) Systems of creation: the emergence of life from nonliving matter. Accounts of Chemical Research 45(12):2131–2141. https://doi.org/10.1021/ar200281t

McCulloch WS, Pitts W (1943) A logical calculus of the ideas immanent in nervous activity. The Bulletin of Mathematical Biophysics 5(4):115–133. https://doi.org/10.1007/BF02478259

Mougkogiannis P, Adamatzky A (2023a) Learning in ensembles of proteinoid microspheres. Royal Society Open Science 10(10):230936. https://doi.org/10.1098/rsos.230936

Mougkogiannis P, Adamatzky A (2023b) Logical gates in ensembles of proteinoid microspheres. PLoS ONE 18(9):e0289433. https://doi.org/10.1371/journal.pone.0289433

Mougkogiannis P, Adamatzky A (2026a) Emergence of periodic oscillations in abiotic proteinoid–neurotransmitter assemblies. ACS Applied Bio Materials 9(16):7326–7356

Mougkogiannis P, Adamatzky A (2026b) Emergent rhythmicity in proteinoid-bz hybrid systems. ACS Synthetic Biology 15(9):3607–3631

Mougkogiannis P, Adamatzky A (2026c) L-theanine proteinoid microspheres as protocognitive systems. Materials Today Chemistry 56:103909

Mougkogiannis P, Nikolaidou A, Adamatzky A (2026) Life-like ferrous oxide microspheres from kombucha. Advanced Materials Interfaces https://doi.org/10.1002/admi.70662

Przybylski AT (1985) Excitable cell made of thermal proteinoids. BioSystems 17(4):281–288. https://doi.org/10.1016/0303-2647(85)90044-9

Przybylski AT, Stratten WP, Syren RM, et al (1982) Membrane, action, and oscillatory potentials in simulated protocells. Naturwissenschaften 69(12):561–563. https://doi.org/10.1007/BF00396351

Qian L, Winfree E (2011) Scaling up digital circuit computation with DNA strand displacement cascades. Science 332(6034):1196–1201. https://doi.org/10.1126/science.1200520

Quiroga RQ, Nadasdy Z, Ben-Shaul Y (2004) Unsupervised spike detection and sorting with wavelets and superparamagnetic clustering. Neural Computation 16(8):1661–1687. https://doi.org/10.1162/089976604774201631

Ruiz-Mirazo K, Briones C, de la Escosura A (2014) Prebiotic systems chemistry: new perspectives for the origins of life. Chemical Reviews 114(1):285–366. https://doi.org/10.1021/cr2004844

Seelig G, Soloveichik D, Zhang DY, et al (2006) Enzyme-free nucleic acid logic circuits. Science 314(5805):1585–1588. https://doi.org/10.1126/science.1132493

Shannon CE (1938) A symbolic analysis of relay and switching circuits. Transactions of the American Institute of Electrical Engineers 57(12):713–723. https://doi.org/10.1109/T-AIEE.1938.5057767

Steinbock O, Kettunen P, Showalter K (1996) Chemical wave logic gates. The Journal of Physical Chemistry 100(49):18970–18975. https://doi.org/10.1021/jp961209v

Tóth Á, Showalter K (1995) Logic gates in excitable media. The Journal of Chemical Physics 103(6):2058–2066. https://doi.org/10.1063/1.469732